Pyonephrosis: Ultrasound and Computed Tomography

Subjects: Urology & Nephrology | Others

Contributor: Stefania Tamburrini

Ultrasound and computed tomography represent the imaging processes of choice in the diagnosis and staging pyonephrosis in emergency settings.

urinary tract infections | CT | US | pyonephrosis | sepsis

1. Introduction

Urinary tract infections (UTIs) are amongst the most frequent community-acquired and healthcare-associated bacterial infections, and they are to be found in many specialties, such as internal medicine, gynecology, urology and intensive care medicine. UTIs are classified based on the anatomical level of infection, the severity grade of infection, underlying risk factors and microbiological findings. However, the clinical phenotypes of UTIs are heterogeneous and range from benign, uncomplicated infections to complicated UTIs (cUTIs), pyelonephritis and severe urosepsis, depending mostly on the host response. Pyonephrosis (PN) refers to infected hydronephrosis with associated suppurative destruction of the kidney parenchyma, with partial or total loss of renal function, and it is defined as an accumulation of purulent debris and sediment in the renal pelvis and urinary collecting system. PN is associated with factors that compromise host defense, including immunosuppression, renal failure, renal transplantation[1][2], and it is associated with local factors that compromise the urinary tract, such as congenital uropathy, neurogenic bladder, pregnancy, presence of foreign bodies such as calculi, indwelling catheters or other drainage devices, or endoscopic maneuvers, and it is frequently associated with the obstruction of the collecting system (renal calculus disease, RCD) [2][3][4][5][6]. PN has also been reported in patients with urinary obstruction from tumors, such as in transitional cell carcinoma[7][8]. Emerging evidence challenges the current paradigm that the bladder is a sterile microenvironment, and reveals that live bacteria are present in the bladder, even in “culture negative” patients[9][10][11][12]. Under basal conditions, the microbiome is not simply an innocent bystander, living peacefully side-by-side with its human host. Rather, commensal microbes are health-promoting and play numerous diverse roles in the maintenance of human wellness. In contrast, the microbiome is altered in multiple disease states with the conversion of the health-inducing microbiome into a disease-promoting microbiome (also known as pathobiome). This condition is particularly pronounced in critically ill patients, where the pathobiome plays an important role in critically ill infection[13][14][15].

Pyonephrosis is uncommon in adults, rare in children and extremely rare in neonates; however, it has been reported in several neonates and adults, making it clear that the condition may develop in any age group. The clinical spectrum of PN is extremely variable, from asymptomatic bacteriuria to sepsis, making diagnosis more

challenging. Similar to an abscess, pyonephrosis is typically associated with fever, chills and flank pain, although some patients may be asymptomatic. The walled-off exudate is protected by the body's natural system and by antibiotics, and for those reasons a prompt diagnosis at an early stage is necessary, because the systemic inflammatory response syndrome leading to major organ dysfunction (fever or hypothermia, hyperleukocytosis or leukopenia, tachycardia, hypotension, tachypnea, neurological compromise (q-SOFA)) is recognized as the first event in a cascade to multi-organ failure. For these reasons, PN is considered a urological emergency that can rapidly progress to sepsis and septic shock[6][16]. The treatment of urosepsis calls for the combination of urgent decompression (either percutaneous or retrograde with a ureteral stent placement under US or CT guidance), adequate life-supporting care, appropriate and prompt antibiotic therapy, and adjunctive measures. Drainage has low morbidity and mortality rates and an excellent outcome, and significantly decreases the need for nephrectomy. The prognosis of pyonephrosis is good in patients who receive prompt diagnosis and treatment, with the infectious process rapidly resolving after either nephrostomy or retrograde stent drainage, because of the adequate control of overwhelming infection in an obstructed renal unit[3][17][18][19][20]. When pyonephrosis is not recognized early, it can rapidly deteriorate and develop into septic shock, and in these cases potential complications include irreversible damage to the kidneys with the possible need for nephrectomy[21]. Ultrasound and computed tomography represent the imaging of choice in the diagnosis and staging of the pathology in emergency settings. In clinical practice the distinction between PN and hydronephrosis is challenging.

Ultrasound is easily performed in emergency settings and bedside for the critically ill patients, and is often used in image guidance for interventions and to monitor the drainage of the calico-pelvic system[3][20][22][23]. Ultrasound can rapidly confirm or exclude the presence of pyonephrosis, speeding up patient management and treatment, and demonstrate hydronephrosis with echogenic debris in the renal pelvis, which is considered highly suggestive of pyonephrosis[18][24][25][26]. Although computed tomography (CT) is considered more reliable, useful, and impactful in the critical care setting[22][23][27][28][29][30][31], the diagnosis can be missed on unenhanced CT because of the difficulty encountered in the radiologic differentiation of hydronephosis from pyonephrosis[31]. The direct assessment of purulent urine is easily performed in the case of the presence of air bubbles; recent studies demonstrated the HU measurement of urine may be helpful in the diagnosis of purulent urine[27][29][30][31]. At contrast-enhanced CT examinations, PN signs are characterized by the presence of signs of obstruction with associated renal pelvic wall thickening and perirenal fat stranding[27][28][32][33].

2. Ultrasound

Renal ultrasound has an established role in evaluating patients with suspected renal inflammatory disease [20][21][34]. Ultrasound is particularly effective in diagnosing pyonephrosis: the sensitivity of renal ultrasonography for differentiating hydronephrosis from pyonephrosis is 90%, and its specificity is 97%[21][24][34]. The key diagnostic point in differentiating urine from infected urine is that in the first case, the collecting system has the acoustic properties of a cystic structure; instead, ultrasonographic findings suggestive of pyonephrosis include the presence of hydronephrosis in conjunction with hyperechoic debris in the collecting system. These findings are specific enough: their absence excludes pyonephrosis with a high degree of accuracy (Figure 1 and Figure 2)[21][24][25][26]

[27][28][35]. In emphysematous pyelonephritis, the presence of gas in the US-B mode is observed as large hyperechoic lines appearing as “dirty shadows” (Figure 3)[36]. US can detect thickening of the renal pelvic wall (>2 mm), which in severe cases may appear multilayered due to mucosa edema (Figure 3). Ultrasonography does have drawbacks [37]; for example, it may not always differentiate hydronephrosis from early pyonephrosis, especially in the case of low-grade hydronephrosis (Figure 4), and the ultrasound diagnosis of PN can be challenging in patients with kidney abnormalities or in the presence of a parapyelic cyst. The major limit of ultrasound is represented by the extrarenal/retroperitoneal extension of the pathology, because of the intrinsic limit of the imaging modality, especially in obese patients. Extrarenal/retroperitoneal extension of pyonephrosis should be considered every time inhomogeneous fluid is seen around the kidney within the perirenal space, in the case of inhomogeneous hyperechogenicity of perirenal fat, or by the direct visualization of extrarenal abscess formation (Figure 5 and Figure 6). In those cases, second level imaging is mandatory to assist the clinician in planning renal decompression.

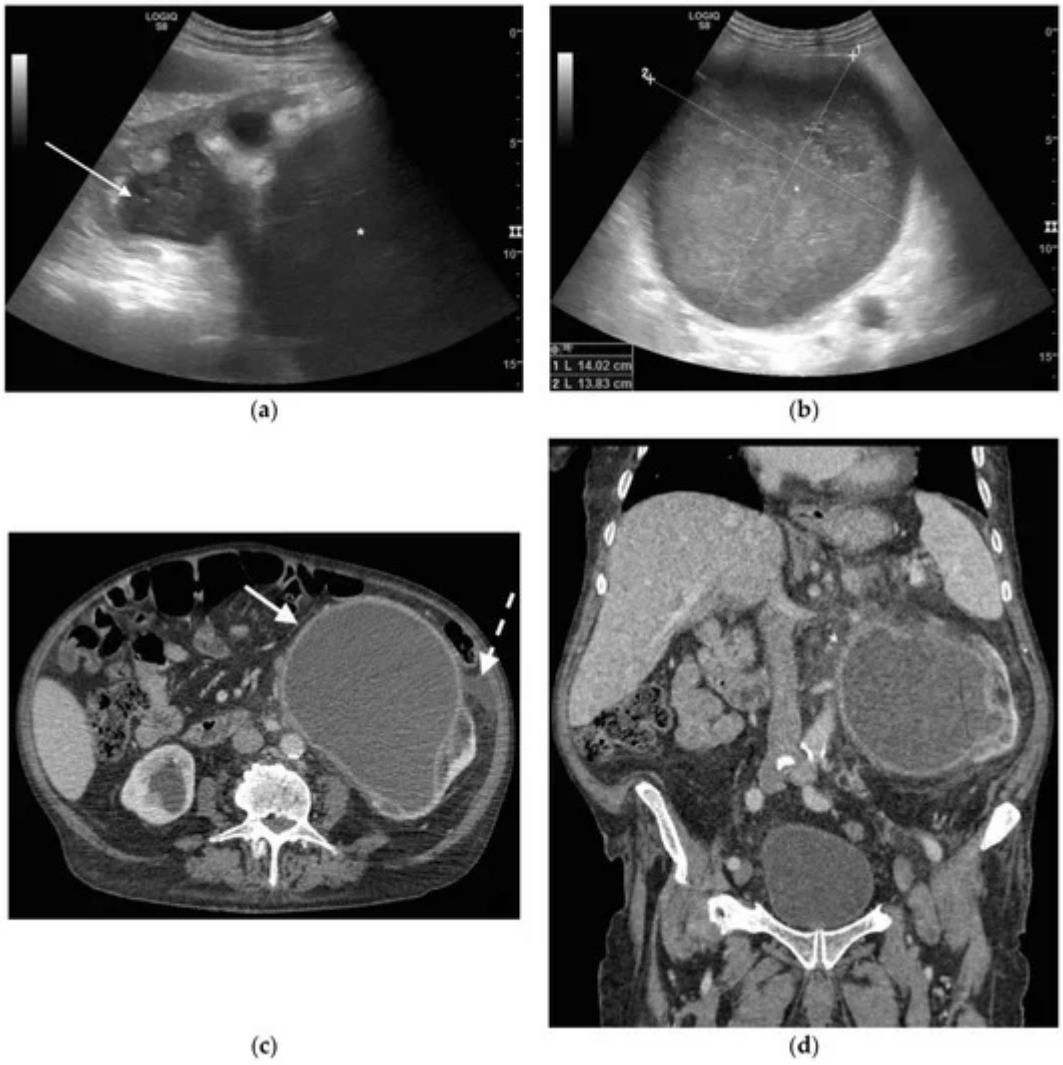

Figure 1. A 78 years old septic male patient. Ultrasound (US) longitudinal (**a**) and axial (**b**) view of the left kidney showing high-grade hydronephrosis with gross dilatation of the renal pelvis and calyces, filled by inhomogeneous urine (white arrow) and an extremely dilated inferior calyceal group filled by a huge ball of debris conglomerate (*).

Axial (**c**) and MPR coronal Computed Tomography (CT) (**d**) after intravenous contrast in cortical-medullary phase, showing high grade hydronephrosis, diffuse parietal thickening of the calico-pelvic system (white arrow), fat stranding of perirenal and renal sinus fat. Small amount of free fluid is appreciated anteriorly (dashed arrow).

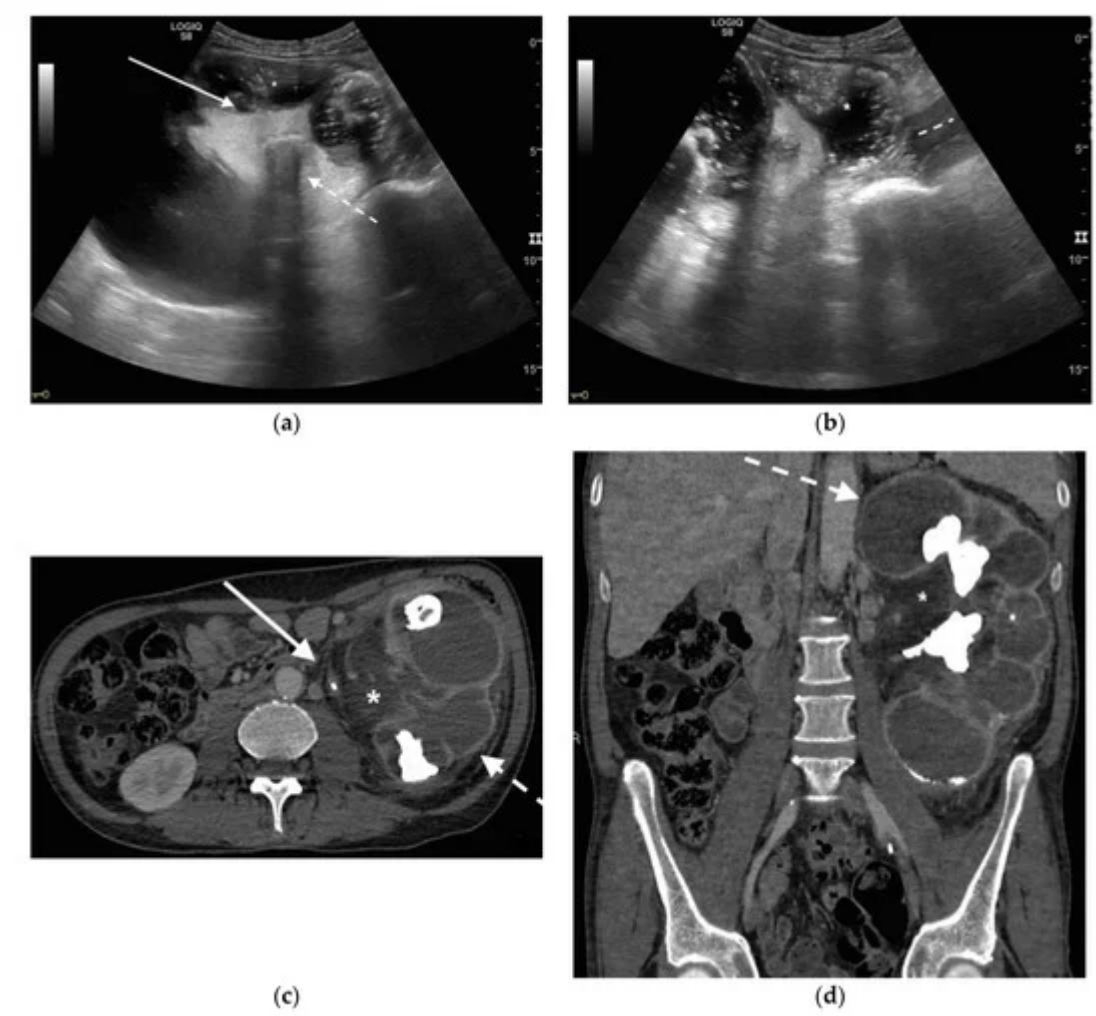

Figure 2. A 71 years old septic patient. US longitudinal (**a**,**b**) view of left kidney. Severe hydronephrosis, with extreme cortical thinning. High-grade dilatation and parietal thickening (white arrow) of calico-pelvic system fluid filled by inhomogeneous fluid with multiple hyperechogenic spots (*). Enlarged and markedly hyperechogenicity of renal sinus fat with acoustic shadowing due to staghorn calculi (dashed arrow). Perirenal fat inhomogeneity was detected (dashed line). Axial (**c**) and MPR coronal (**d**) CT with intravenous contrast in cortical-medullary phase after stent placement (white arrow), showing high-grade hydronephrosis with diffuse parietal thickening of calico-pelvic system (dashed arrow), staghorn calculi and renal sinus lipomatosis with mild inhomogeneous fat stranding and suffusion (*).

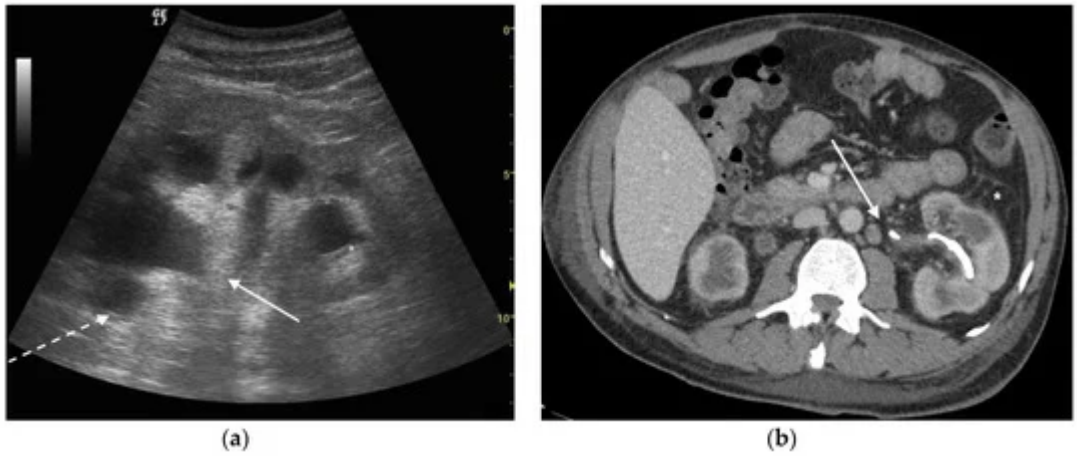

Figure 3. A 73 years old septic male patient. US longitudinal view of left kidney (**a**,**b**) showing hydronephrosis with parietal thickening of inferior calyceal group (*), dense peripheral echoes within the calyceal system (white arrow) with acoustic shadowing at low-gain indicating gas-forming infection, perirenal suffusion was detected (dashed arrow). Axial CT (**b**) with intravenous contrast in cortical-medullary phase after stent placement (white arrow), showing drainage of calico-pelvic system. Mild perirenal fat stranding (*).

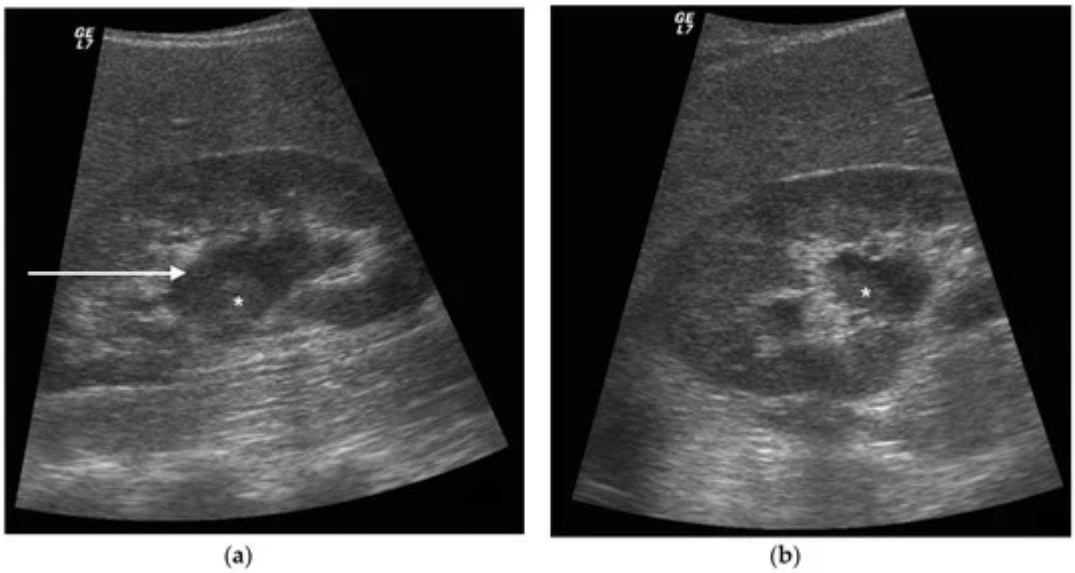

Figure 4. A 42 years old septic female patient. US longitudinal view (**a**,**b**) of the right kidney showing low/mild-grade hydronephrosis (white arrow) with sharply defined urine debris level (*).

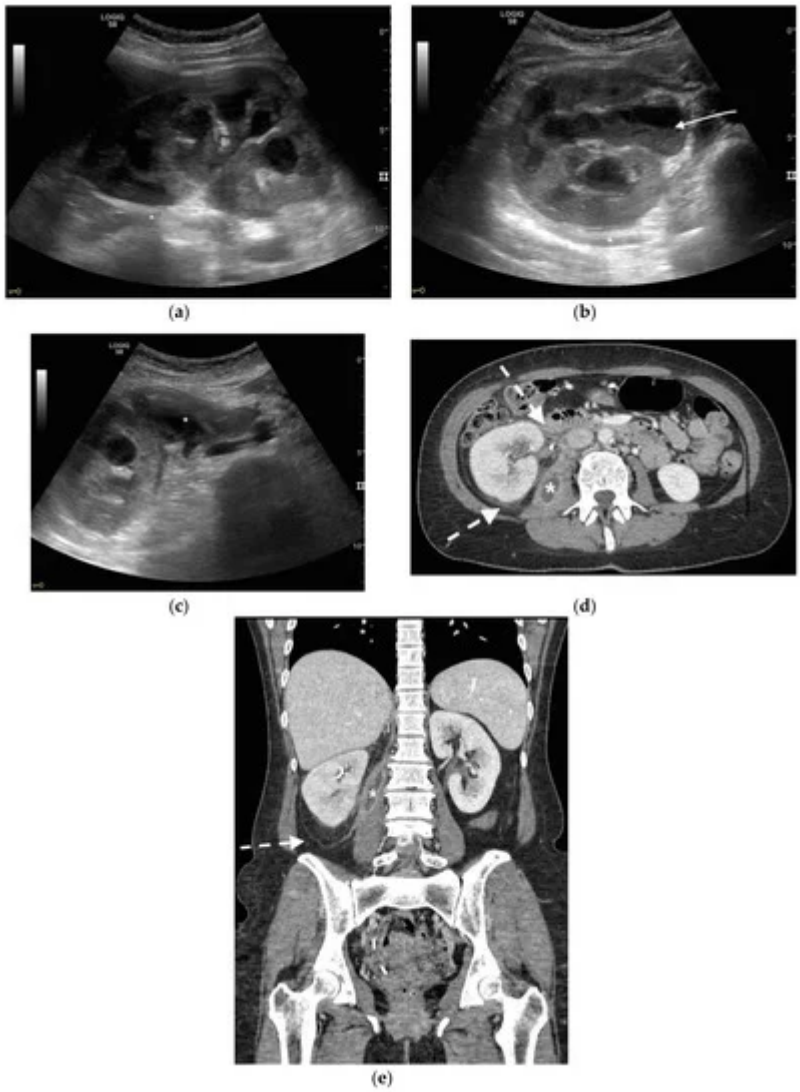

Figure 5. A 48 years old septic woman. US longitudinal (**a**) and axial (**b**,**c**) view of the right kidney. Enlargement of the kidney, hydronephrosis with sharply defined urine-debris level (white arrow). Thickening of perirenal fascia and markedly inhomogeneous echogenicity of perirenal fat suggesting extrarenal extension (*). The patient underwent nephrostomy in the emergency setting, and CT was performed after stent placement. Axial (**d**) and MPR coronal (**e**) CT with intravenous contrast in parenchymal phase, showing correct stent positioning (white arrow) and drainage of calyceal-pelvic system. The right kidney appeared enlarged with a delayed parenchymal phase, the calyceal-pelvic system was unstretched after nephrostomy placement. Right perirenal fascia was thickened posteriorly (dashed arrow) and extrarenal extension of the pathology was confirmed by the presence of an abscess in the right iliopsoas muscle (*).

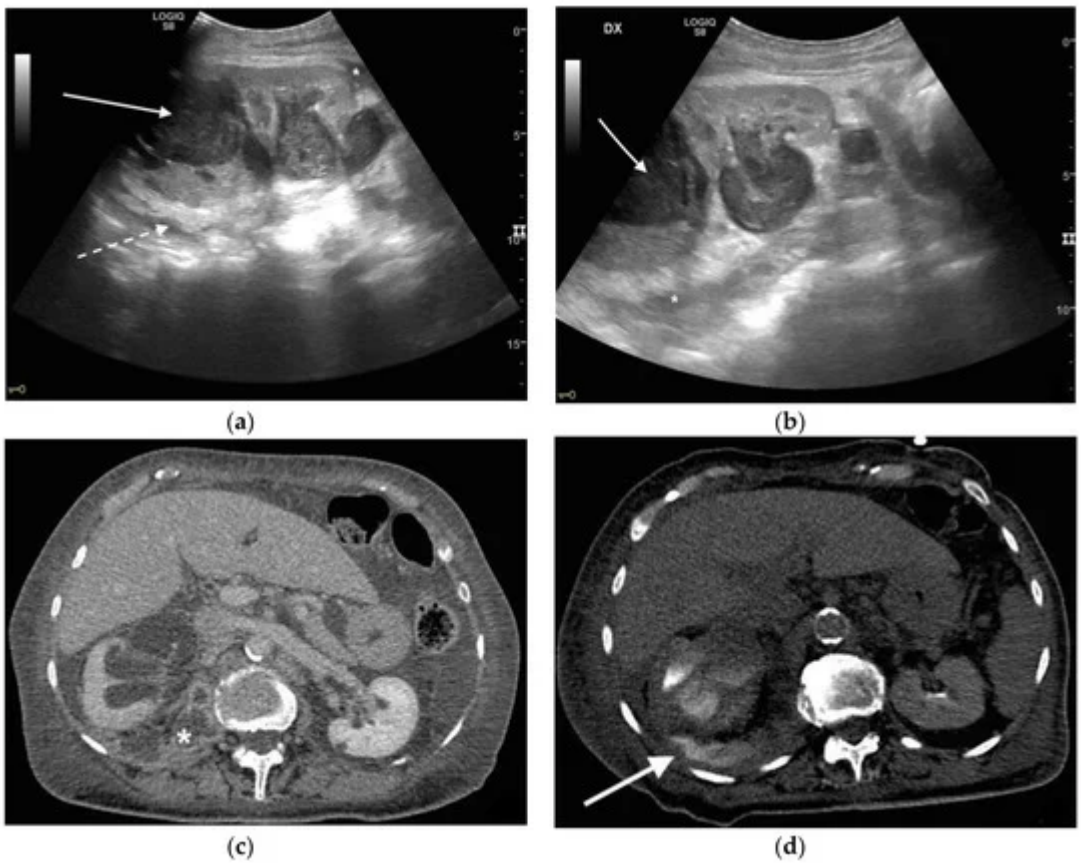

Figure 6. An 83 years old septic woman. US longitudinal (**a**,**b**) view of the right kidney showing high-grade hydronephrosis with the calyceal-pelvic system completely occupied by inhomogeneous echogenic debris (with arrow). Perirenal fascia is thickened and perirenal fat is hyperechogenic and inhomogeneous (dashed arrow). Fluid over-collection is appreciated around the kidney (*), and free fluid was appreciated in the abdomen. Complicated pyonephrosis with extrarenal extension was diagnosed. CT with intravenous contrast. Axial CT after intravenous contrast in parenchymal (**c**) and urography phase (**d**), showing hydronephrosis with parietal thickening of calyceal-pelvic system, multiple loculated over fluid collection in the perirenal (white arrow) space and abscess in iliopsoas muscle (*). In the urography phase, extravasation of urine into extrarenal fluid collections due to abscessualization of the calyceal-pelvic system.

References

1. Flores-Mireles, A.L.; Walker, J.N.; Caparon, M.G.; Hultgren, S.J. Urinary tract infections: Epidemiology, mechanisms of infection and treatment options. Nat. Rev. Microbiol. 2015, 13, 269–284.
2. Wagenlehner, F.M.E.; Johansen, T.E.B.; Cai, T.; Koves, B.; Kranz, J.; Pilatz, A.; Tandogdu, Z. Epidemiology, definition and treatment of complicated urinary tract infections. Nat. Rev. Urol. 2020, 17, 586–600.

3. Wagenlehner, F.M.E.; Pilatz, A.; Weidner, W.; Naber, K.G. Urosepsis: Overview of the Diagnostic and Treatment Challenges. Microbiol. Spectr. 2015, 3.
4. Wang, X.; Tang, K.; Xia, D.; Peng, E.; Li, R.; Liu, H.; Chen, Z. A novel comprehensive predictive model for obstructive pyonephrosis patients with upper urinary tract stones. Int. J. Clin. Exp. Pathol. 2020, 13, 2758–2766.
5. Patodia, M.; Goel, A.; Singh, V.; Singh, B.P.; Sinha, R.J.; Kumar, M.; Dalela, D.; Sankhwar, S.N. Are there any predictors of pyonephrosis in patients with renal calculus disease? Urolithiasis 2017, 45, 415–420.
6. Nicola, R.; Menias, C.O. Urinary Obstruction, Stone Disease, and Infection. In Diseases of the Abdomen and Pelvis 2018–2021: Diagnostic Imaging-IDKD Book; Hodler, J., Kubik-Huch, R.A., von Schulthess, G.K., Eds.; Springer International Publishing: Cham, Switzerland, 2018; pp. 223–228.
7. Li, H.; Xie, F.; Zhao, C.; Yi, Z.; Chen, J.; Zu, X. Primary mucinous adenocarcinoma of the renal pelvis misdiagnosed as calculous pyonephrosis: A case report and literature review. Transl. Androl. Urol. 2020, 9, 781–788.
8. Chen, L.; Li, J.-X.; Huang, X.-B.; Wang, X.-F. Analysis for risk factors of systemic inflammatory response syndrome after one-phase treatment for apyrexic calculous pyonephrosis by percutaneous nephrolithotomy. Beijing Da Xue Xue Bao Yi Xue Ban 2014, 46, 566–569.
9. Lewis, D.A.; Brown, R.; Williams, J.; White, P.; Jacobson, S.K.; Marchesi, J.R.; Drake, M.J. The human urinary microbiome; bacterial DNA in voided urine of asymptomatic adults. Front. Cell. Infect. Microbiol. 2013, 3, 41.
10. Siddiqui, H.; Lagesen, K.; Nederbragt, A.J.; Jeansson, S.L.; Jakobsen, K.S. Alterations of microbiota in urine from women with interstitial cystitis. BMC Microbiol. 2012, 12, 205.
11. Nelson, D.E.; Van Der Pol, B.; Dong, Q.; Revanna, K.V.; Fan, B.; Easwaran, S.; Sodergren, E.; Weinstock, G.M.; Diao, L.; Fortenberry, J.D. Characteristic Male Urine Microbiomes Associate with Asymptomatic Sexually Transmitted Infection. PLoS ONE 2010, 5, e14116.
12. Dong, Q.; Nelson, D.E.; Toh, E.; Diao, L.; Gao, X.; Fortenberry, J.D.; Van Der Pol, B. The Microbial Communities in Male First Catch Urine Are Highly Similar to Those in Paired Urethral Swab Specimens. PLoS ONE 2011, 6, e19709.
13. Alverdy, J.C.; Krezalek, M.A. Collapse of the Microbiome, Emergence of the Pathobiome, and the Immunopathology of Sepsis. Crit. Care Med. 2017, 45, 337–347.
14. Fay, K.T.; Ford, M.L.; Coopersmith, C.M. The intestinal microenvironment in sepsis. Biochim. Biophys. Acta Mol. Basis Dis. 2017, 1863 Pt B, 2574–2583.

15. Klingensmith, N.J.; Coopersmith, C.M. The Gut as the Motor of Multiple Organ Dysfunction in Critical Illness. Crit. Care Clin. 2016, 32, 203–212.
16. Florido, C.; Herren, J.L.; Pandhi, M.B.; Niemeyer, M.M. Emergent Percutaneous Nephrostomy for Pyonephrosis: A Primer for the On-Call Interventional Radiologist. Semin. Interv. Radiol. 2020, 37, 74–84.
17. Thornton, R.H.; Covey, A.M. Urinary Drainage Procedures in Interventional Radiology. Tech. Vasc. Interv. Radiol. 2016, 19, 170–181.
18. Flukes, S.; Hayne, D.; Kuan, M.; Wallace, M.; McMillan, K.; Rukin, N.J. Retrograde ureteric stent insertion in the management of infected obstructed kidneys. BJU Int. 2015, 115 (Suppl. 5), 31–34.
19. Chang, C.W.; Huang, C.N. Pyonephrosis drained by double-J catheter. Clin. Case Rep. 2020, 8, 3586–3587.
20. Shifti, D.M.; Bekele, K. Generalized peritonitis after spontaneous rupture of pyonephrosis: A case report. Int. Med. Case Rep. J. 2018, 11, 113–116.
21. Colemen, B.G.; Arger, P.H.; Mulhern, C.B., Jr.; Pollack, H.M.; Banner, M.P. Pyonephrosis: Sonography in the diagnosis and management. AJR Am. J. Roentgenol. 1981, 137, 939–943.
22. Manno, E.; Navarra, M.; Faccio, L.; Motevallian, M.; Bertolaccini, L.; Mfochive, A.; Pesce, M.; Evangelista, A. Deep impact of ultrasound in the intensive care unit: The “ICU-sound” protocol. Anesthesiology 2012, 117, 801–809.
23. Narasimhan, M.; Koenig, S.J.; Mayo, P.H. A Whole-Body Approach to Point of Care Ultrasound. Chest 2016, 150, 772–776.
24. Kamboj, M.; Loy, J.L.; Koratala, A. Renal ultrasonography: A reliable diagnostic tool for pyonephrosis. Clin. Case Rep. 2018, 6, 1176–1178.
25. Subramanyam, B.R.; Raghavendra, B.N.; Bosniak, M.A.; Lefleur, R.S.; Rosen, R.J.; Horii, S.C. Sonography of pyonephrosis: A prospective study. AJR Am. J. Roentgenol. 1983, 140, 991–993.
26. Gupta, R.; Gupta, S.; Choudhary, A.; Basu, S. Giant Pyonephrosis Due to Ureteropelvic Junction Obstruction: A Case Report. J. Clin. Diagn. Res. 2017, 11, PD17–PD18.
27. Demertzis, J.; Menias, C.O. State of the art: Imaging of renal infections. Emerg. Radiol. 2007, 14, 13–22.
28. Browne, L.P.; Mason, E.O.; Kaplan, S.L.; Cassady, C.I.; Krishnamurthy, R.; Guillerman, R.P. Optimal imaging strategy for community-acquired Staphylococcus aureus musculoskeletal infections in children. Pediatr. Radiol. 2008, 38, 841–847.
29. Basmaci, I.; Sefik, E. A novel use of attenuation value (Hounsfield unit) in non-contrast CT: Diagnosis of pyonephrosis in obstructed systems. Int. Urol. Nephrol. 2020, 52, 9–14.

30. Boeri, L.; Fulgheri, I.; Palmisano, F.; Lievore, E.; Lorusso, V.; Ripa, F.; D'Amico, M.; Spinelli, M.G.; Salonia, A.; Carrafiello, G.; et al. Hounsfield unit attenuation value can differentiate pyonephrosis from hydronephrosis and predict septic complications in patients with obstructive uropathy. Sci. Rep. 2020, 10, 18546.
31. Yuruk, E.; Tuken, M.; Sulejman, S.; Colakerol, A.; Serefoglu, E.C.; Sarica, K.; Muslumanoglu, A.Y. Computerized tomography attenuation values can be used to differentiate hydronephrosis from pyonephrosis. World J. Urol. 2017, 35, 437–442.
32. Kawashima, A.; Leroy, A.J. Radiologic evaluation of patients with renal infections. Infect. Dis. Clin. N. Am. 2003, 17, 433–456.
33. Zulfiqar, M.; Ubilla, C.V.; Nicola, R.; Menias, C.O. Imaging of Renal Infections and Inflammatory Disease. Radiol. Clin. N. Am. 2020, 58, 909–923.
34. Vourganti, S.; Agarwal, P.K.; Bodner, D.R.; Dogra, V.S. Ultrasonographic Evaluation of Renal Infections. Radiol. Clin. N. Am. 2006, 44, 763–775.
35. Hansen, K.L.; Nielsen, M.B.; Ewertsen, C. Ultrasonography of the Kidney: A Pictorial Review. Diagnostics 2015, 6, 2.
36. Joseph, R.C.; Amendola, M.A.; Artze, M.E.; Casillas, J.; Jafri, S.Z.; Dickson, P.R.; Morillo, G. Genitourinary tract gas: Imaging evaluation. Radiographics 1996, 16, 295–308.
37. Chung, S.-D.; Lai, M.-K.; Chueh, S.-C.; Wang, S.-M.; Yu, H.-J. An unusual cause of pyonephrosis and intra-peritoneal abscess: Ureteral urothelial carcinoma. Int. J. Infect. Dis. 2009, 13, e39–e40.